

# Engineering Elasticity and Relaxation Time in Metal-Coordinate Cross-Linked Hydrogels

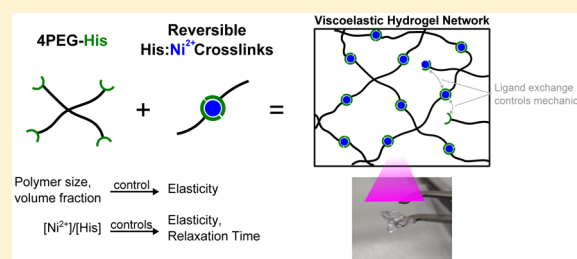
Scott C. Grindy,<sup>†</sup> Martin Lenz,<sup>‡</sup> and Niels Holten-Andersen<sup>\*,†</sup>

<sup>†</sup>Department of Materials Science and Engineering, Massachusetts Institute of Technology, Cambridge, Massachusetts 02139, United States

<sup>‡</sup>Laboratoire de Physique Théorique et Modèles Statistiques (LPTMS), CNRS, Université Paris-Sud, Université Paris-Saclay, 91405 Orsay, France

## S Supporting Information

**ABSTRACT:** Reversible cross-links between polymer chains are a promising avenue to engineer the mechanical properties of soft materials and in particular hydrogels. Such developments are however challenged by the complexity of these materials, which unlike conventional, permanently cross-linked gels involve multiple relaxation time scales. To address this challenge, we study a model system of tetra-arm poly(ethylene glycol) hydrogels transiently cross-linked by reversible histidine: $\text{Ni}^{2+}$  coordinate complexes and explore the separate influences of polymer structure and cross-link density on the time-dependent hydrogel rheology. We show that the characteristics of the polymer matrix primarily control the hydrogels' static elasticity, implying that its dynamics are largely governed by coordinate-bond rearrangement kinetics rather than polymer relaxation time scales. By contrast, the ion concentration has a strong influence on both the hydrogel's statics and dynamics, and we quantitatively account for the former using a simple model based on the known equilibrium bonding properties of histidine: $\text{Ni}^{2+}$  complexes. Our findings establish specific engineering principles for the viscoelastic mechanics of metal-coordinate hydrogel materials, thus opening new perspectives for the optimization of their use in (bio)functional applications.



## INTRODUCTION

Hydrogels have shown promise in biocompatible applications such as synthetic tissues, injectable wound-healing materials, and in drug delivery.<sup>1,2</sup> However, conventional, covalent hydrogels can be weak and brittle, and a large body of recent research has therefore focused on improving upon their mechanical properties.<sup>3–12</sup> A key thrust of this field is the creation of and control over energy-dissipating mechanisms within the hydrogel network structure. One strategy for achieving this goal is to create hydrogels with a large number of dynamic network interactions<sup>8</sup> via hydrogen bonds, ionic clusters, hydrophobic associations, metal–ligand complexes, host–guest complexes, biological receptor–ligand complexes, or dynamic covalent bonds. These developments call for a better understanding of the interplay between reversible cross-link mechanics and mesoscale dynamics in determining the time scale and magnitude of macroscopic viscoelastic energy dissipation in these materials.

Recently, we and others have addressed this challenge using a system of hydrogels composed of 4-arm poly(ethylene glycol) (4PEG) cross-linked by metal–ligand interactions<sup>13–16</sup> inspired by marine mussels.<sup>17–21</sup> Specifically, we use model 4-arm poly(ethylene glycol) polymers functionalized with a histidine moiety (4PEG-His). When mixed with transition metal ions at physiologic pH, the His: Metal complexes will function as transient cross-links between polymers. In the proper concentration range, a hydrogel is formed (Figure 1), and the His: Metal

bonds allow extensive control over the hydrogels' mechanical properties.<sup>18,21–25</sup> Because of the transient nature of the His: Metal complexes, 4PEG-His hydrogels are viscoelastic rather than just elastic. The corresponding mechanical relaxation time can vary over several orders of magnitude depending on which metallic ion is used to form the transient cross-link junctions, while the plateau modulus is largely unaffected.<sup>18,21</sup>

In this paper, we further explore these transient network hydrogels from an engineering perspective, comparing the level of control gained using conventional polymer engineering to that associated with the specific metal-coordinate exchange dynamics. Indeed, while the influence of polymer dynamics in the viscoelasticity of transient networks is well studied,<sup>26–37</sup> less attention has been paid to the effect of stoichiometry between associating groups. Most theories thus consider either –AA– type homocomplementary associations, where two or more identical functional groups form an association, or –AB– type heterocomplementary associations, where two or more chemically distinct groups form an association.

By contrast, metal-coordinate bonds can be multivalent, with up to six ligands binding a single metal ion.<sup>38</sup> Our specific His: $\text{Ni}^{2+}$  metal-coordinate cross-links thus involve complexes of

Received: July 14, 2016

Revised: October 11, 2016

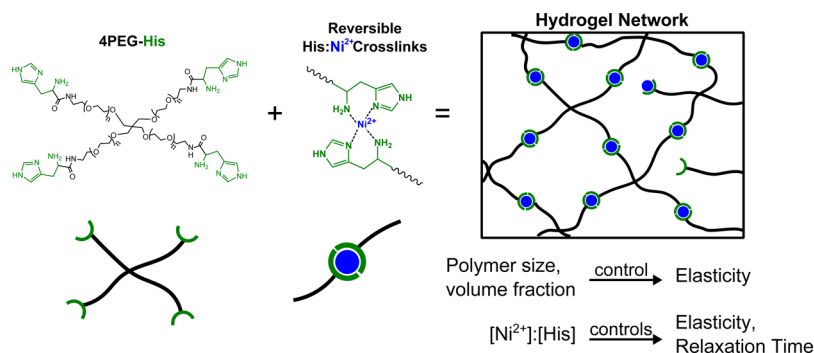


**Figure 1.** Our model system is composed of 4-arm poly(ethylene glycol); the end of each arm is functionalized with an N-terminal histidine residue (4PEG-His). We synthesize the hydrogels by mixing a pH 7.4-buffered 4PEG-His solution with aqueous  $\text{Ni}^{2+}$  ions. The strong yet reversible  $\text{Ni}^{2+}$ :His interactions cross-link the polymers, resulting in a viscoelastic hydrogel.

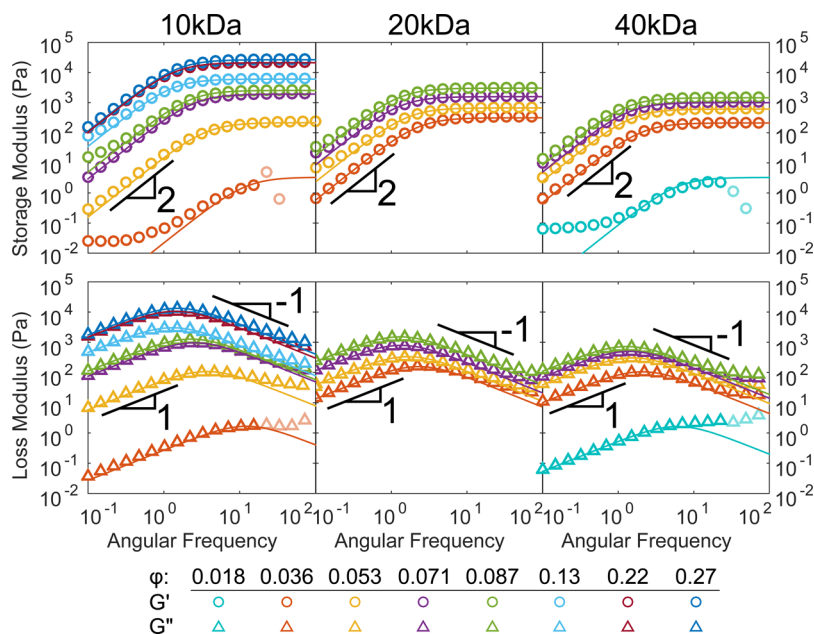


**Figure 2.** Linear rheology of our hydrogels is well described by a simple Maxwell model with two materials parameters: plateau modulus  $G_p$  and relaxation time  $\tau$  (solid lines). Both  $G_p$  and  $\tau$  generally increase with increasing volume fraction  $\phi$ . All measurements shown are at 20 °C. Faded data points in low- $\phi$  data indicate probable machine errors.

the form  $-\text{AB}$ ,  $-\text{ABA}-$ , and  $(-\text{A})_3\text{B}$ ,<sup>18</sup> where a multifunctional cross-linker B binds up to three polymer-bound  $-\text{A}$  groups. As the cross-linker concentration can be controlled independently from the polymer concentration in the system, both overstoichiometric or understoichiometric cross-linker concentrations can be used to provide additional control in comparison to conventional polymer materials.

In the current study, we use His- $\text{Ni}^{2+}$  complexes as a model cross-link to explore the time-dependent response of tetra-PEG transient networks as characterized by their plateau modulus  $G_p$  and viscoelastic terminal relaxation time  $\tau$ . We show that the plateau modulus can be selectively controlled over several orders of magnitude using the conventional polymer materials engineering knobs of concentration and molecular weight. By contrast, the  $\text{Ni}^{2+}$ :His ratio strongly influences both  $G_p$  and  $\tau$ . Finally, the plateau modulus and relaxation time exhibit clear maxima near a stoichiometric ratio of  $\text{Ni}^{2+}$ :His = 1:3, suggesting that three-coordinated complexes are essential contributors to the hydrogel's material properties.

## METHODS

All reagents were purchased from Sigma-Aldrich unless otherwise noted.

**Synthesis of 4PEG-His.** 4PEG-His was synthesized using appropriate modifications of the procedure by Fullenkamp et al.<sup>18</sup> Briefly,  $\sim 1\text{--}5$  g of 4-arm PEG- $\text{NH}_2\cdot\text{HCl}$  (0.25 equiv of PEG, 1.0 equiv of  $-\text{NH}_2$  groups) (JenKem USA) was mixed with Boc-His(Trt)-OH (1.5 equiv) and BOP reagent (1.5 equiv) and dissolved in  $\sim 15$  mL of dichloromethane. *N,N*-Diisopropylethylamine (DIPEA) (535 equiv) was added, and the reaction was allowed to proceed for 2 h under  $\text{N}_2$ . The product was purified by precipitation in diethyl ether 1 $\times$ , methanol at  $-20$  °C 3 $\times$ , and diethyl ether 1 $\times$  and then vacuum-dried. Protecting groups were removed by a cleavage solution of 95 mL of trifluoroacetic acid, 2.5 mL of triisopropylsilane, and 2.5 mL of  $\text{H}_2\text{O}$  for 2 h. The solvent was removed under reduced pressure, and the product was purified by redissolving in methanol, precipitation in ether 3 $\times$ , and vacuum drying.

To confirm the incorporation of histidine onto the PEG polymer, polymers were dissolved in  $\text{CDCl}_3$  and  $^1\text{H}$  NMR spectra were taken on a Bruker AVANCE-400 MHz spectrometer and processed using MestReNova software. Chemical shift values are reported in ppm relative to trimethylsilane, shown in Figures S3 and S4. Chemical shifts at ca. 7.45, 8.5, and 8.65 confirm incorporation of the histidine onto 4PEG- $\text{NH}_2$ .

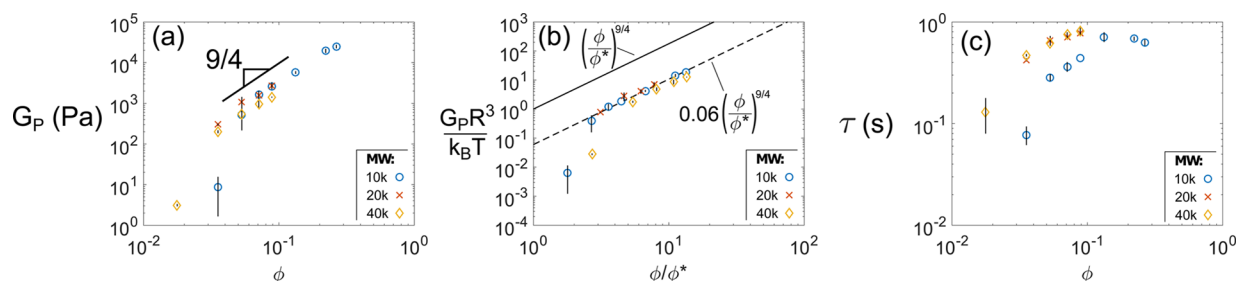


**Figure 3.** Examining how the modulus and relaxation time depend on 4PEG-His volume fraction  $\phi$  provide hints at the mechanisms controlling the mechanical properties. (a)  $G_p$  displays a power-law dependence with  $\phi$  above the polymer overlap volume fraction. (b) The collapse of the data on to the dimensionless modulus  $\bar{G}_p = G_p R^3 / k_B T \propto (\phi / \phi^*)^{9/4}$  (solid line) suggests that the network elasticity is controlled by the polymer correlation length. The actual dependence  $\bar{G}_p = \mu (\phi / \phi^*)^{9/4}$  however involves a small prefactor  $\mu = 0.06$  (dashed line). (c) While the modulus varies over several decades in the volume fractions studied here, the relaxation time  $\tau$  is much less sensitive to 4PEG-His concentration. All measurements shown are at 20 °C. Error bars show standard deviation.

**Hydrogel Formation.** Hydrogels were formed by mixing appropriate volumes of (1) 200 mg/mL solution of 4PEG-His in Milli-Q H<sub>2</sub>O, (2) 1.0 M phosphate buffer at pH 7.4, (3) Milli-Q H<sub>2</sub>O, and (4) aqueous solution of NiCl<sub>2</sub>·6H<sub>2</sub>O. The final buffer concentration was 0.2 M in all hydrogels in this work. Upon adding the Ni<sup>2+</sup> solution, gelation was observed nearly instantaneously at the site of injection. Samples were thoroughly homogenized by vortex mixing, centrifuged for 5 min to remove air bubbles, and stored at 5 °C for at least 12 h prior to characterization.

**Rheological Characterization.** All rheological characterizations were carried out on an Anton Paar MCR 302 stress-controlled rheometer using a 25 mm diameter cone–plate geometry with a 1° cone angle and a 51 μm truncation. Samples were loaded at room temperature and then cooled to 5 °C while undergoing preshear at  $\dot{\gamma} = 1 \text{ s}^{-1}$  for 10 min. The samples then rested ( $\dot{\gamma} = 0 \text{ s}^{-1}$ ) for 5 min. Frequency sweeps were conducted at  $\gamma_0 = 5\%$ , well within the linear viscoelastic range (Figure S2), at 5, 10, 15, 20, and 25 °C. Experimental moduli were fitted to the Maxwell model:  $G' = G_p \omega^2 \tau^2 / (1 + \omega^2 \tau^2)$  and  $G'' = G_p \omega \tau / (1 + \omega^2 \tau^2)$  using a log-weighted nonlinear least-squares fitting method.

**Estimation of Polymer Parameters.** In order to rescale our findings across molecular weights and concentrations, we use the parameters for poly(ethylene glycol) in Tripathi et al.<sup>32</sup> The Kuhn length  $a$  and number of Kuhn segments  $n$  are calculated using

$$a = \frac{C_\infty l}{\sin(\theta)} \quad (1a)$$

$$n = \frac{3M_W \sin^2(\theta)}{M_0 C_\infty} \quad (1b)$$

where  $M_W$  is the molecular weight of the polymer,  $C_\infty = 4$ ,  $l = 0.154 \text{ nm}$  is the carbon–carbon bond length,  $M_0 = 44 \text{ g/mol}$  is the molecular mass of the PEG repeat unit, and  $\theta = 54.5^\circ$  is the half-angle between carbon–carbon bonds. This results in  $a = 0.757 \text{ nm}$  and  $n = M_W / (88.5 \text{ g/mol})$ .

We estimate the free chain relaxation time of our polymers, assuming semidilute unentangled chains as<sup>39</sup>

$$\tau_{\text{chain}} \approx \frac{\eta_s a^3 n^2 \phi^{0.31}}{k_B T} \quad (2)$$

where  $\eta_s$  is the viscosity of water  $\approx 1 \text{ mPa}\cdot\text{s}$  and  $a$  is the aforementioned Kuhn length. In the case of 10 kDa polymers ( $N = 137$ ) at  $\phi = 0.1$  and  $T = 20 \text{ °C}$ , we estimate  $\tau_{\text{chain}} \approx 1 \times 10^{-6} \text{ s}$ , significantly lower than our observed relaxation times of  $\sim 0.5 \text{ s}$ .

## RESULTS AND DISCUSSION

**Polymer Concentration and Molecular Weight Primarily Control Elasticity.** We used oscillatory rheology to measure the frequency-dependent storage modulus  $G'(\omega)$  and loss modulus  $G''(\omega)$  at a series of molecular weights of 4PEG-His (10, 20, and 40 kDa) and volume fractions ( $\phi = 0.018\text{--}0.266$ ,

corresponding to 2–30 wt %), initially using a constant Ni<sup>2+</sup>:His ratio of 1:2. These moduli directly relate to parameters  $G_p$  and  $\tau$ , which are respectively defined as the storage modulus at infinite frequency  $G'(\omega \rightarrow \infty)$  and the inverse of the frequency where  $G'(\omega)$  becomes larger than  $G''(\omega)$ . As shown in Figure 2, both  $G_p$  and  $\tau$  generally increase with increasing polymer volume fraction  $\phi$ , indicating the formation of gels of increasing cohesiveness. We extract the parameters  $G_p$  and  $\tau$  by fitting a Maxwell model to our data, yielding excellent agreement across most of the measured frequency regime. While there is some deviation at the extremes of the frequency regime which indicates the presence of other characteristic time scales,<sup>16</sup> a single modulus  $G_p$  and terminal relaxation time  $\tau$  describe the majority of the rheological properties, and importantly fitting our data to a Maxwell model allows us a consistent method for estimating our hydrogels' primary relaxation time and the corresponding modulus.

To elucidate the influence of the polymer matrix on the hydrogel's material properties, we quantitatively investigate the influence of its molecular weight and concentration on the viscoelastic parameters  $G_p$  and  $\tau$  (Figure 3). This influence is very substantial on the plateau modulus, which varies over several orders of magnitude over the range studied (Figure 3a). For moderate to high polymer volume fractions, the dependence of the plateau modulus on  $\phi$  appears compatible with a power law. For low values of  $\phi$  ( $\leq 0.036\text{--}0.053$  at 10 kDa,  $\leq 0.018\text{--}0.036$  at 40 kDa), this dependence breaks down and gels become very weak, with storage and loss moduli several orders of magnitude below those of hydrogels at higher polymer concentrations. Additionally, while most samples exhibit terminal relaxation behavior at frequencies below  $1/\tau$  ( $G' \propto \omega^2$  and  $G'' \propto \omega^1$  as shown in Figure 2), the samples at low  $\phi$  do not follow terminal scaling.

We hypothesize that this sudden loss of rigidity marks the connectivity percolation threshold, below which bonding between polymers is too sparse for a rigid system-spanning gel to form. This percolation threshold corresponds to volume fractions of the order of the overlap volume fraction  $\phi^*$ , where the average distance between two polymer coils equals their typical size. We compute  $\phi^* = na^3/R^3$ , where  $n$  is the number of Kuhn segments in a chain,  $a$  is the size of these segments, and  $R = \sqrt{\langle R^2 \rangle} = n^{3/5}a$  gives the typical size of a coil in a good solvent (see Methods for details on calculations). The resulting values,  $\phi^* = 0.070$  at 10 kDa and  $\phi^* = 0.023$  at 40 kDa, are compatible with our observations and thus support our interpretation of the observed rigidity transition.

Focusing on the data collected above the transition, we observe that the relaxation time scale of the gel is of order 500 ms and relatively constant, covering about half a decade without any clear scaling (Figure 3c). In contrast, the observed plateau moduli span over 2 decades over the same range of  $\phi$ . This comparatively weak  $\phi$  dependence of the relaxation time suggests that it is essentially determined by the detachment kinetics of the gel's coordinate cross-links, as opposed to polymer relaxation. Indeed, for the polymers in our study's conditions we estimate the relaxation times of semidilute unentangled chains to be roughly  $\tau_{\text{chain}} \approx 10^{-6}$  s (see Methods section for details), several orders of magnitude faster than the observed relaxation times in Figures 2 and 3.<sup>39</sup> This suggests that chain relaxation is much faster than the network rearrangement process, and therefore the viscoelastic relaxation process is most likely controlled by the Ni:His exchange kinetics, which explains the comparatively weak  $\phi$  dependence of  $\tau$ . This is corroborated by the previously documented dependence of the viscoelastic time scale on the identity of the coordinated metal.<sup>18,20,21</sup>

Turning to the behavior of  $G_p$  above the rigidity transition, we observe that it has a strong  $\phi$  dependence, namely  $G_p \propto \phi^{9/4}$ , reminiscent of elastic regimes governed by the polymer correlation length  $\xi = a\phi^{-3/4}$ .<sup>40</sup> The role of the correlation length can be understood by considering a polymer chain in a semidilute ( $\phi > \phi^*$ ) solution: over distances smaller than  $\xi$ , the surroundings of any point of the chain are overwhelmingly occupied by monomers of the same chain, with the probability of encountering other chains comparatively low. Over larger length scales, encounters with other chains become predominant. When applying these considerations to conventional permanently cross-linked semidilute gels, we expect chains to entangle over a typical length scale  $\xi$ . Such gels therefore typically comprise one elastically active "effective chain" per volume  $\xi^3$ , endowing them with an elastic modulus  $G_p^{\text{permanent}} \approx k_B T / \xi^3$ , or equivalently

$$\tilde{G}_p = G_p R^3 / k_B T \approx (\phi / \phi^*)^{9/4} \quad (3)$$

Testing the prediction of eq 3 in Figure 3b, we find a good collapse of our data in terms of its dimensionless variables and a very good agreement with the predicted scaling. We however observe that the magnitude of  $G_p$  in our measurements is much smaller than predicted:  $G_p^{\text{measured}} = \mu G_p^{\text{permanent}}$  with  $\mu = 0.06$ .

Although the plateau modulus scaling we observe of  $G_p \propto \phi^{9/4}$  corresponds to the classical expectation for an entangled polymer system, the effects of entanglements may not be applicable in all conditions studied here, especially in the concentrations near the rigidity transition, and it is possible another mechanism could lead to a similar dependence. The transient bonding present in our system implies that their behavior should differ significantly from classically entangled gels, since all entanglement constraints could be released through His:Ni<sup>2+</sup> bond rearrangement rather than through reptation. It is possible that entanglements or some related mechanism also help to explain the relatively small value of  $\mu$  (part of which may be explained by loops and any systematic errors in our naive estimates for  $R^2$ ). Overall, while our theoretical understanding of the gels' transient microstructure and dynamics is still speculative and will be refined in upcoming work, our data are consistent with a collection of effective chains of size  $\propto \xi$  connected by transient coordinate cross-links.

**Metal/Ligand Ratio Defines a Window of Highly Tunable Stiffness and Relaxation Time.** As discussed previously, most of the work on polymer networks with reversible interactions does not focus on off-stoichiometry systems, where either functional groups or cross-linkers are in

excess of the other. Therefore, we decided to conduct a systematic investigation of the effects of Ni<sup>2+</sup>:His concentration ratios on the viscoelastic properties of our 4PEG-His:Ni<sup>2+</sup> system by making a series of 20 kDa gels at constant  $\phi = 0.071$ , with Ni<sup>2+</sup>:His ratios from 1:4 to 1:1. Across all measured Ni<sup>2+</sup>:His ratios, the mechanical properties maintain their Maxwellian shape, as indicated in Figure 4. While there is deviation from

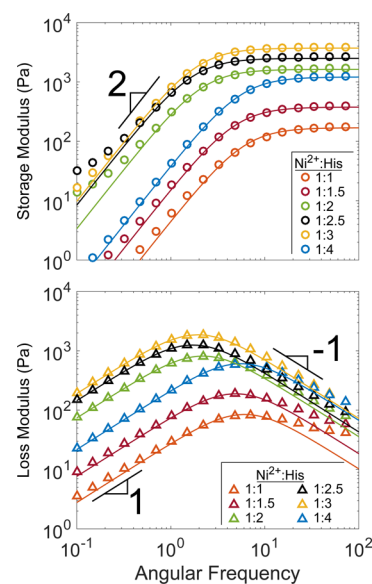


**Figure 4.** Oscillatory rheology of 4PEG-His:Ni<sup>2+</sup> hydrogels at varying Ni<sup>2+</sup>:His ratios show nonmonotonic scaling of  $\tau$  and  $G_p$ , showing that the network connectivity determines both the plateau modulus and relaxation time. 20 kDa hydrogels are shown at 25 °C,  $\phi = 0.071$ . The 1:1 Ni<sup>2+</sup>:His gels are only nominally 1:1. As shown in Figure S1, some of the Ni<sup>2+</sup> precipitated out from the solution, and as such the effective ratio of Ni<sup>2+</sup>:His is lower than 1:1; these gels represent the maximum solubility of Ni<sup>2+</sup> in the hydrogel.

Maxwell-like behavior in  $G''$  at high frequencies, similar to the previous section the Maxwell model effectively allows us to estimate the primary relaxation time and its corresponding modulus. The fitted  $G_p$  and  $\tau$  strongly depend on Ni<sup>2+</sup>:His ratios, indicating that the network connectivity influences both mechanical parameters (Figure 5b,c). We further note that the plateau modulus is maximal for a 1:3 Ni<sup>2+</sup>:His stoichiometry. This observation is initially surprising, as it implies that decreasing the concentration of Ni<sup>2+</sup>:His cross-links from the 1:2 situation described in the last section stiffens the gel rather than weakens it. Furthermore, previous research found that the mechanical properties of terpyridine (tpy)-based metallosupramolecular polymers were maximized at a 1 metal:2 ligands molar ratio.<sup>15,41</sup> In particular, Schmatloch and Schubert<sup>41</sup> found that the viscosity of linear 2PEG-tpy:Zn<sup>2+</sup> is maximal at Zn<sup>2+</sup>:tpy = 1:2; studying 4PEG-tpy, Rossow et al.<sup>15</sup> found that  $G_p$  is maximized at Zn<sup>2+</sup>:tpy = 1:2. This contrasts with our findings in Figures 4 and 5, where we find a maximum  $G_p$  at Ni<sup>2+</sup>:His = 1:3. We believe this difference can be attributed to the structural differences between tpy and His complexes: tpy typically forms tpy<sub>2</sub>M<sup>2+</sup> complexes, while the histidine analogue histamine (having both the primary amine nitrogen and imidazole nitrogens as coordination sites) can form up to His<sub>3</sub>Ni<sup>2+</sup> complexes.<sup>38</sup>

To understand the dependence of  $G_p$  on Ni<sup>2+</sup>/His ratio, we model the different types of cross-link species that may form

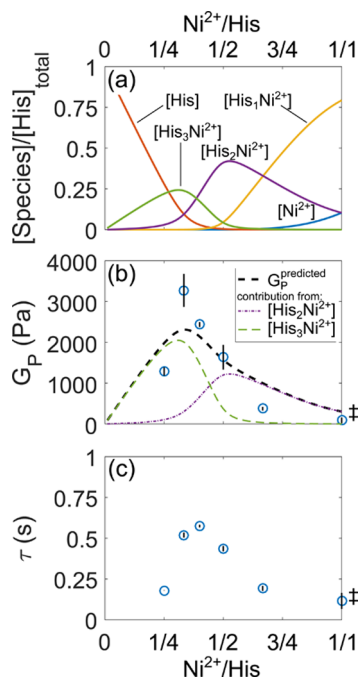
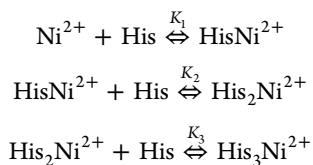


**Figure 5.** Influence of Ni<sup>2+</sup>:His stoichiometry on hydrogel mechanical properties. (a) We use the equilibrium constants of histamine:Ni<sup>2+</sup> complexes to estimate the concentrations of His<sub>*n*</sub>Ni<sup>2+</sup> species. (b) Combining the estimations in (a) with the mechanical characterization of Figure 4 through the model of eq 5 allows us to account for the dependence of the plateau modulus on stoichiometry. We also break down the contributions to G<sub>p</sub><sup>predicted</sup> from His<sub>2</sub>Ni<sup>2+</sup>- and His<sub>3</sub>Ni<sup>2+</sup>-type cross-links. (c) The relaxation time τ is largest at Ni<sup>2+</sup>:His = 1:2.5, suggesting an interplay of several relaxation mechanisms. All the data for 20 kDa 4PEG-His gels are shown at 25 °C and φ = 0.071. Error bars show standard deviations. †The 1:1 Ni<sup>2+</sup>:His gels are only nominally 1:1 as some of the Ni<sup>2+</sup> precipitated out from the solution (Figure S1).

across the different Ni<sup>2+</sup>:His ratios. Our model thus considers several His<sub>*n*</sub>Ni<sup>2+</sup> complexes where *n* histidines bind Ni<sup>2+</sup>. We consider the following chemical equilibria:



and use previously measured equilibrium constants<sup>38</sup> for histamine:Ni<sup>2+</sup> complexes  $K_1 = 10^{6.82} \text{ M}^{-1}$ ,  $K_2 = 10^{5.05} \text{ M}^{-1}$ , and  $K_3 = 10^{3.12} \text{ M}^{-1}$ . We expect these constants to be good approximations of the equilibria associated with our His:Ni<sup>2+</sup> complexes due to the resemblance of the histamine and histidine coordination motifs, with chelation from both the primary amine nitrogen and imidazole nitrogen to the Ni<sup>2+</sup> ions. Crucially, these equilibrium constants allow for the formation of three-coordinated complexes (His<sub>3</sub>Ni<sup>2+</sup>) for low Ni<sup>2+</sup> concentrations. We compute the concentrations of His<sub>*n*</sub>Ni<sup>2+</sup> complexes across the range of Ni<sup>2+</sup>:His concentration ratios we employed experimentally and display our results in Figure 5a. In practice, these concentrations are insensitive to the values of the equilibrium constants as long as  $K_1 \gg K_2 \gg K_3 \gg 1/[\text{His}]_{\text{total}}$  where  $[\text{His}]_{\text{total}} = [\text{His}] + [\text{HisNi}^{2+}] + 2[\text{His}_2\text{Ni}^{2+}] + 3[\text{His}_3\text{Ni}^{2+}]$  stands for the total concentration of ligands in the gel. As Figure 5 shows, this calculation reveals that while the Ni<sup>2+</sup>:His = 1:2 gels used in the previous section predominantly involved

His<sub>2</sub>Ni<sup>2+</sup> complexes, other stoichiometries result in substantial concentrations of coordinate complexes with potentially different contributions to the gel's elasticity.

To predict the different His:Ni<sup>2+</sup> complexes' contributions to the gel's plateau modulus, we note that each (effective) elastically active chain discussed in the previous section contributes a quantity  $\approx k_B T$  to the gel's elastic energy extrapolated to unit strain. We furthermore reason that while His<sub>2</sub>Ni<sup>2+</sup> complexes connect two 4PEG and therefore participate in at most one elastically active chain, His<sub>3</sub>Ni<sup>2+</sup> complexes can participate in three elastic chains as schematized in Figure 6. Conversely,

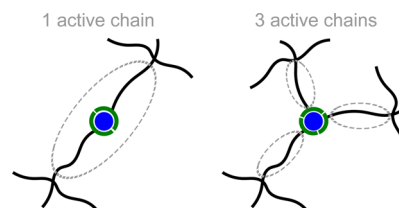


**Figure 6.** While the formation of a His<sub>2</sub>Ni<sup>2+</sup> complex creates one elastically active chain, a His<sub>3</sub>Ni<sup>2+</sup> complex creates three elastically active chains (dashed ellipses). Therefore, His<sub>3</sub>Ni<sup>2+</sup> complexes contribute proportionally more to the elastic modulus as reflected in eq 4.

isolated Ni<sup>2+</sup> ions and HisNi<sup>2+</sup> complexes do not contribute to elasticity. This reasoning thus suggests that the elastic contribution of a His<sub>3</sub>Ni<sup>2+</sup> complex is 3 times larger than that of a His<sub>2</sub>Ni, implying

$$G_p^{\text{predicted}} \propto \frac{[\text{His}_2\text{Ni}^{2+}] + 3[\text{His}_3\text{Ni}^{2+}]}{[\text{His}]_{\text{total}}} \quad (4)$$

Using the results of the φ and molecular weight scaling in Figure 3b, we determine the proportionality constant in eq 4 to be equal to 2μG<sub>p</sub><sup>permanent</sup>, with μ = 0.06 (the factor of 2 ensures consistency with eq 3). We thus obtain

$$G_p^{\text{predicted}} = \frac{2([\text{His}_2\text{Ni}^{2+}] + 3[\text{His}_3\text{Ni}^{2+}]) \mu k_B T}{[\text{His}]_{\text{total}} R^3} \left( \frac{\phi}{\phi^*} \right)^{9/4} \quad (5)$$

As shown in Figure 5b, this simple prediction without adjustable parameters accounts for the experimentally observed variations of the plateau modulus. Note that this prediction does not account for the shift in the bond percolation threshold in situations where free ions and one-coordinated HisNi<sup>2+</sup> complexes are prevalent, causing an overprediction of the modulus for relatively large Ni<sup>2+</sup>:His ratios.

Despite its limitations, our naive model captures the observation that the stiffest hydrogels are obtained at Ni<sup>2+</sup>:His ratios of 1:3 (Figure 5b) because His<sub>3</sub>Ni<sup>2+</sup> complexes act as additional branching points in the gel. The relaxation time τ of our gels, on the other hand, is longest at slightly lower Ni<sup>2+</sup>:His ratio of 1:2.5 and is overall less sensitive than G<sub>p</sub> to the Ni<sup>2+</sup>:His ratio. We speculate that this dependence could be the result of the interplay of two ligand dissociation processes in His<sub>3</sub>Ni<sup>2+</sup>-containing gels: a relatively fast dissociation of these complexes into His<sub>2</sub>Ni<sup>2+</sup> and a slower subsequent decay into elastically inactive HisNi<sup>2+</sup>.

Another factor which could affect the relaxation time is the presence of freely mobile ligands, which we and co-workers have recently shown can strongly affect the dynamics of linear polymer systems.<sup>25</sup> At Ni<sup>2+</sup>:His ≈ 1/3–1/2, there is a minimum of [His]

and  $[\text{HisNi}^{2+}]$ . The presence of these relatively mobile species could accelerate the rate of network remodeling, decreasing the relaxation time.

## CONCLUSIONS

This is not the first study to characterize hydrogel mechanics dominated by mussel-inspired metal-coordinate cross-link dynamics. However, while past studies have been focused on exploring coordinate cross-link dynamic control via choice of pH, metal ion, or ligand design,<sup>17–21,42,43</sup> here we instead characterize the separate influences of coordinate cross-link density and dynamics on gel viscoelastic mechanics. We show that the plateau modulus of 4PEG-His: $\text{Ni}^{2+}$  hydrogels scales with polymer concentration and size in similar ways to analogous covalently cross-linked hydrogel systems, indicating that cross-link density primarily controls the hydrogels' static elasticity. By contrast, the concentration of  $\text{Ni}^{2+}$  is found to strongly influence both the hydrogel's statics and dynamics with the most rigid networks centered at a  $\text{Ni}^{2+}$ :His ratio of 1:3 and not 1:2, as used in previous studies.<sup>18</sup> We quantitatively account for this observation using a simple model based on coordinate cross-link topological effects on local network mechanics. Furthermore, we note that Fullenkamp et al.<sup>18</sup> upon changing pH of 4PEG-His: $\text{Ni}^{2+}$  hydrogels similarly describe a peak in relaxation time, which could be caused by the same model we propose here.

In conclusion, our findings should be broadly relevant for future engineering of hydrogel viscoelastic mechanics using metal-coordinate cross-link dynamics. We confirm that hydrogel mechanics are largely governed by coordinate-bond rearrangement dynamics rather than polymer relaxation time scales. Additionally, we expand the metal-coordinate cross-link-based toolkit for hydrogel viscoelastic control further beyond conventional engineering strategies such as polymer concentration and size. Specifically, we demonstrate that simply adjusting the concentration of the coordinating metal ion allows easy tuning of both gel plateau modulus and relaxation time.

## ASSOCIATED CONTENT

### Supporting Information

The Supporting Information is available free of charge on the ACS Publications website at DOI: 10.1021/acs.macromol.6b01523.

Figures S1–S4 (PDF)

## AUTHOR INFORMATION

### Corresponding Author

\*E-mail: [holten@mit.edu](mailto:holten@mit.edu) (N.H.-A.).

### Notes

The authors declare no competing financial interest.

## ACKNOWLEDGMENTS

Financial support of this work by the Office of Naval Research (ONR) under the Young Investigators Program Grant ONR N00014-15-1-2763 is gratefully acknowledged. S.C.G. and N.H.A. were supported in part by the MRSEC Program of the National Science Foundation under Award DMR-1419807. M.L. was supported by Marie Curie Integration Grant PCIG12-GA-2012-334053, "Investissements d'Avenir" LabEx PALM (ANR-10-LABX-0039-PALM), ANR grant ANR-15-CE13-0004-03, and ERC Starting Grant 677532. M.L.'s group belongs to the CNRS consortium CellTiss. N.H.A. and M.L. were supported in

part by the MIT-France program of the MIT International Science and Technology Initiatives (MISTI).

## REFERENCES

- (1) Kopecek, J. Hydrogel biomaterials: a smart future? *Biomaterials* **2007**, *28*, 5185–92.
- (2) Thiele, J.; Ma, Y.; Bruekers, S. M. C.; Ma, S.; Huck, W. T. S. 25th Anniversary Article: Designer Hydrogels for Cell Cultures: A Materials Selection Guide. *Adv. Mater.* **2014**, *26*, 125–148.
- (3) Henderson, K. J.; Zhou, T. C.; Otim, K. J.; Shull, K. R. Ionically Cross-Linked Triblock Copolymer Hydrogels with High Strength. *Macromolecules* **2010**, *43*, 6193–6201.
- (4) Gong, J.; Katsuyama, Y.; Kurokawa, T.; Osada, Y. Double-Network Hydrogels with Extremely High Mechanical Strength. *Adv. Mater.* **2003**, *15*, 1155–1158.
- (5) Gong, J. P. Why are double network hydrogels so tough? *Soft Matter* **2010**, *6*, 2583.
- (6) Sun, J.-Y.; Zhao, X.; Illeperuma, W. R. K.; Chaudhuri, O.; Oh, K. H.; Mooney, D. J.; Vlassak, J. J.; Suo, Z. Highly stretchable and tough hydrogels. *Nature* **2012**, *489*, 133–6.
- (7) Hao, J.; Weiss, R. Mechanical behavior of hybrid hydrogels composed of a physical and a chemical network. *Polymer* **2013**, *54*, 2174–2182.
- (8) Zhao, X. Multi-scale multi-mechanism design of tough hydrogels: building dissipation into stretchy networks. *Soft Matter* **2014**, *10*, 672–687.
- (9) Lin, S.; Cao, C.; Wang, Q.; Gonzalez, M.; Dolbow, J. E.; Zhao, X. Design of stiff, tough and stretchy hydrogel composites via nanoscale hybrid crosslinking and macroscale fiber reinforcement. *Soft Matter* **2014**, *10*, 7519–7527.
- (10) Haque, M. A.; Kurokawa, T.; Gong, J. P. Super tough double network hydrogels and their application as biomaterials. *Polymer* **2012**, *53*, 1805–1822.
- (11) Shams Es-haghi, S.; Leonov, A. I.; Weiss, R. A. Deconstructing the Double-Network Hydrogels: The Importance of Grafted Chains for Achieving Toughness. *Macromolecules* **2014**, *47*, 4769–4777.
- (12) Shibayama, M. Structure-mechanical property relationship of tough hydrogels. *Soft Matter* **2012**, *8*, 8030.
- (13) Hackelbusch, S.; Rossow, T.; van Assenbergh, P.; Seiffert, S. Chain Dynamics in Supramolecular Polymer Networks. *Macromolecules* **2013**, *46*, 6273–6286.
- (14) Rossow, T.; Seiffert, S. Supramolecular polymer gels with potential model-network structure. *Polym. Chem.* **2014**, *5*, 3018–3029.
- (15) Rossow, T.; Habicht, A.; Seiffert, S. Relaxation and Dynamics in Transient Polymer Model Networks. *Macromolecules* **2014**, *47*, 6473–6482.
- (16) Tang, S.; Habicht, A.; Li, S.; Seiffert, S.; Olsen, B. D. Self-Diffusion of Associating Star-Shaped Polymers. *Macromolecules* **2016**, *49*, 5599–5608.
- (17) Holten-Andersen, N.; Harrington, M. J.; Birkedal, H.; Lee, B. P.; Messersmith, P. B.; Lee, K. Y. C.; Waite, J. H. pH-induced metal-ligand cross-links inspired by mussel yield self-healing polymer networks with near-covalent elastic moduli. *Proc. Natl. Acad. Sci. U. S. A.* **2011**, *108*, 2651–5.
- (18) Fullenkamp, D. E.; He, L.; Barrett, D. G.; Burghardt, W. R.; Messersmith, P. B. Mussel-Inspired Histidine-Based Transient Network Metal Coordination Hydrogels. *Macromolecules* **2013**, *46*, 1167–1174.
- (19) Menyo, M. S.; Hawker, C. J.; Waite, J. H. Versatile tuning of supramolecular hydrogels through metal complexation of oxidation-resistant catechol-inspired ligands. *Soft Matter* **2013**, *9*, 10314–10323.
- (20) Holten-Andersen, N.; Jaishankar, A.; Harrington, M. J.; Fullenkamp, D. E.; DiMarco, G.; He, L.; McKinley, G. H.; Messersmith, P. B.; Lee, K. Y. C. Metal-coordination: using one of nature's tricks to control soft material mechanics. *J. Mater. Chem. B* **2014**, *2*, 2467–2472.
- (21) Grindy, S. C.; Learsch, R.; Mozhdzhi, D.; Cheng, J.; Barrett, D. G.; Guan, Z.; Messersmith, P. B.; Holten-Andersen, N. Control of hierarchical polymer mechanics with bioinspired metal-coordination dynamics. *Nat. Mater.* **2015**, *14*, 1210–1216.

- (22) Mozhdehi, D.; Ayala, S.; Cromwell, O. R.; Guan, Z. Self-Healing Multiphase Polymers via Dynamic Metal-Ligand Interactions. *J. Am. Chem. Soc.* **2014**, *136*, 16128–16131.
- (23) Pham, T. T. H.; van der Gucht, J.; Mieke Kleijn, J.; Cohen Stuart, M. A. Reversible polypeptide hydrogels from asymmetric telechelics with temperature-dependent and Ni<sup>2+</sup>-dependent connectors. *Soft Matter* **2016**, *12*, 4979–4984.
- (24) Wegner, S. V.; Schenk, F. C.; Witzel, S.; Bialas, F.; Spatz, J. P. Cobalt Cross-Linked Redox-Responsive PEG Hydrogels: From Viscoelastic Liquids to Elastic Solids. *Macromolecules* **2016**, *49*, 4229–4235.
- (25) Mozhdehi, D.; Neal, J. A.; Grindy, S. C.; Cordeau, Y.; Ayala, S.; Holtén-Andersen, N.; Guan, Z. Tuning Dynamic Mechanical Response in Metallopolymer Networks through Simultaneous Control of Structural and Temporal Properties of the Networks. *Macromolecules* **2016**, *49*, 6310–6321.
- (26) Rubinstein, M.; Semenov, A. N. Thermoreversible Gelation in Solutions of Associating Polymers. 2. Linear Dynamics. *Macromolecules* **1998**, *31*, 1386–1397.
- (27) Rubinstein, M.; Semenov, A. N. Dynamics of Entangled Solutions of Associating Polymers. *Macromolecules* **2001**, *34*, 1058–1068.
- (28) Green, M. S.; Tobolsky, A. V. A New Approach to the Theory of Relaxing Polymeric Media. *J. Chem. Phys.* **1946**, *14*, 80.
- (29) Tanaka, F.; Edwards, S. Viscoelastic properties of physically crosslinked networks. 1. Transient network theory. *Macromolecules* **1992**, *25*, 1516–1523.
- (30) Annable, T.; Buscall, R.; Ettelaie, R.; Whittlestone, D. The rheology of solutions of associating polymers: Comparison of experimental behavior with transient network theory. *J. Rheol.* **1993**, *37*, 695.
- (31) Marrucci, G.; Bhargava, S.; Cooper, S. L. Models of shear-thickening behavior in physically crosslinked networks. *Macromolecules* **1993**, *26*, 6483–6488.
- (32) Tripathi, A.; Tam, K. C.; McKinley, G. H. Rheology and Dynamics of Associative Polymers in Shear and Extension: Theory and Experiments. *Macromolecules* **2006**, *39*, 1981–1999.
- (33) Xu, D.; Craig, S. L. Scaling laws in supramolecular polymer networks. *Macromolecules* **2011**, *44*, 5465–5472.
- (34) Appel, E. A.; Forster, R. A.; Koutsioubas, A.; Toprakcioglu, C.; Scherman, O. A. Activation Energies Control the Macroscopic Properties of Physically Cross-Linked Materials. *Angew. Chem., Int. Ed.* **2014**, *53*, 10038–10043.
- (35) Loveless, D. M.; Jeon, S. L.; Craig, S. L. Rational Control of Viscoelastic Properties in Multicomponent Associative Polymer Networks. *Macromolecules* **2005**, *38*, 10171–10177.
- (36) Yount, W. C.; Loveless, D. M.; Craig, S. L. Small-molecule dynamics and mechanisms underlying the macroscopic mechanical properties of coordinatively cross-linked polymer networks. *J. Am. Chem. Soc.* **2005**, *127*, 14488–96.
- (37) Yount, W. C.; Loveless, D. M.; Craig, S. L. Strong means slow: dynamic contributions to the bulk mechanical properties of supramolecular networks. *Angew. Chem., Int. Ed.* **2005**, *44*, 2746–8.
- (38) Sjöberg, S. Critical evaluation of stability constants of metal-imidazole and metal-histamine systems (Technical Report). *Pure Appl. Chem.* **1997**, *69*, 1549–1570.
- (39) Rubinstein, M.; Colby, R. H. *Polymer Physics*; OUP Oxford: 2003; p 456.
- (40) de Gennes, P.-G. *Scaling Concepts in Polymer Physics*; Cornell University Press: Ithaca, NY, 1979.
- (41) Schmatloch, S.; Schubert, U. Engineering with metallo-supramolecular polymers: linear coordination polymers and networks. *Macromol. Symp.* **2003**, *199*, 483–498.
- (42) Menyo, M. S.; Hawker, C. J.; Waite, J. H. Rate-Dependent Stiffness and Recovery in Interpenetrating Network Hydrogels through Sacrificial Metal Coordination Bonds. *ACS Macro Lett.* **2015**, *4*, 1200–1204.
- (43) Barrett, D. G.; Fullenkamp, D. E.; He, L.; Holtén-Andersen, N.; Lee, K. Y. C.; Messersmith, P. B. pH-Based Regulation of Hydrogel Mechanical Properties Through Mussel-Inspired Chemistry and Processing. *Adv. Funct. Mater.* **2013**, *23*, 1111–1119.